International Journal of Scientific Engineering and Applied Science (IJSEAS) – Volume-4, Issue-02, February 2018
ISSN: 2395-3470
www.ijseas.com

Application of the ionic character percentage calculation in raw materials selection for nonhydrolytic sol-gel heterogeneous polycondensation to form M-O-M' bond

Guo Feng [a,*], Weihui Jiang [a, b, *], Jianmin Liu [a], Qing Shao [b], Quan Zhang [a]

a National Engineering Research Center for Domestic & Builing Ceramics, Jingdezhen Ceramic Institute, Jingdezhen 333000, China

b Department of Material Science and Engineering, Jingdezhen Ceramic Institute, Jingdezhen 333000, China

Abstract

Heterogeneous M-O-M' bond formation in the precursor gel is the key to the low temperature synthesis of multicomponent oxides via sol-gel method. The heterogeneous polycondensation reaction of nonhydrolytic sol-gel method provides a simple and facile way to form heterogeneous M-O-M' bond in the gel. However, not all raw materials can ensure the formation of M-O-M' bond in nonhydrolytic heteropolycondensation reaction. This paper gives a brief discussion on the nucleophilic substitution mechanism and process of nonhydrolytic sol-gel heterogeneous polycondensation reaction, combined with our specific case analysis, it is found that the selection of raw materials should first meet the need to nonhydrolytic polycondensation reaction mechanism. Meanwhile, the raw materials M-A and M'–B should have high covalent character (namely low ionic character percentage) to ensure the metal base can replace the leaving group after the nucleophile’s nucleophillic attack, so as to ensure the formation of M-O-M' bond in the gel.

1. Introduction

Nonhydrolytic sol-gel method directly takes the polycondensation reaction from the precursor to gel without the hydrolysis process (see Arnal, Corriu, Leclercq, And, & Vioux, 1997; Joo, Kwon, Yu, & Hyeon, 2005; Vioux, 1997). It simplifies the technological process without the hydrolysis rate controlling of the precursor. More importantly, nonhydrolytic sol-gel method is used to form heterogeneous M-O-M' bond, which makes it easier to achieve uniform atomistic mixing and greatly reduce the synthesis temperature of multicomponent oxides (see Andrianainarivelo, Corriu, Leclercq, And, & Vioux, 1997; Vona, Polini, Sebastianelli, & Licoccia, 2004). However, the formation of M-O-M' bond is also closely related to the selection of raw materials in practical application.

Meanwhile, when atoms form a covalent bond, it is often between the covalent and ionic bond, which belongs to the covalent-ionic bond. Estimation the ionic character percentage of bond is a common problem in inorganic chemistry (see Isotani, & Watari, 1976; Warhurst, 1951). Although it is difficult to calculate the quantitative relationship of the ionic character of the covalent bond accurately and it is still an unsatisfactory problem, there are some empirical rules that can be referred to (see Fajans, 1941; Pauling, 1932; Isotani, & Watari, 1976; Warhurst, 1951).

This paper gives a brief review on nonhydrolytic sol-gel heterogeneous polycondensation reaction. Combining with the review on the nucleophilic substitution reaction process of nonhydrolytic heterogeneous polycondensation, this paper summarizes the basic principle for raw materials selection to form M-O-M' bond in gel via nonhydrolytic sol-gel method. This paper also analyzes our specific application cases of the ionic character the percentage calculation in raw materials selection for nonhydrolytic sol-gel heterogeneous polycondensation to form M-O-M' bond.

2. Experimental procedure

2.1 Preparation of samples

2.1.1 Samples preparation for cordierite synthesis

Homemade anhydrous aluminium ethoxide ($Al(OEt)_3$) was first prepared by using aluminum powder (Al, AR, Shanghai) and anhydrous ethanol (EtOH, AR, Shanghai) as raw materials, and iodide (I_2, AR, Shanghai) as catalyzer (see Feng, Jiang, Liu, Li, Zhang, Miao, & Wu, 2017). Then, corresponding amount of tetraethoxysilane ($Si(OEt)_4$, AR, Shanghai) was added and refluxed at 80 ℃ for 24 h. And then magnesium sources of anhydrous magnesium chloride ($MgCl_2$, AR, Shanghai) ($M_1^{\#}$) and magnesium acetate ($Mg(OOCCH_3)_2$, AR, Shanghai) ($M_2^{\#}$) was added, respectively. And the mixture was placed in the vessel at 110 ℃ for 24 h to get the gel. Finally, the gel was ground and calcined at 1200 ℃ for 2 h (see Feng, Jiang, Liu, Zhang, Wu, & Miao, 2017).

2.1.2 Samples preparation for magnesium-stabilized aluminum titanate synthesis

To synthesize magnesium-stabilized aluminum titanate, anhydrous aluminum chloride ($AlCl_3$, AR, Shanghai), titanium tetrachloride ($TiCl_4$, AR, Shanghai) were used as precursors and anhydrous ethanol (EtOH, AR, Shanghai) was used as oxygen donor, anhydrous magnesium fluoride (MgF_2, AR, Shanghai), anhydrous magnesium acetate ($Mg(OOCCH_3)_2$, AR, Shanghai) and magnesium ethoxide ($Mg(OH_2CCH_3)_2$, AR, Shanghai) were used to investigate the effect of magnesium sources on the stabilization effect of aluminum titanate. $AlCl_3$, EtOH and $TiCl_4$ were mixed in a conical flask with the nominal composition of Al_2TiO_5. The reaction mixture was continuously refluxed at 110 ℃ for 8 h to obtain the aluminum titanate wet gel via nonhydrolytic sol-gel process. The wet gel was dissoluted with $CHCl_3$ solution of magnesium fluoride ($M_1^{\#}$), magnesium ethoxide ($M_2^{\#}$) and magnesium acetate ($M_3^{\#}$). And the doping amount of magnesium sources was 10 mol % (mole ratio to aluminum titanate). And then the mixture was refluxed at 110 ℃ for 12 h. It was dried at 110 ℃, ground and calcined at 750 ℃ for 2 h to obtain samples (see Feng, Jiang, Liu, Zhang, Hu, & Miao, 2016; Feng, Jiang, Liu, Zhang, Hu, & Miao, 2017).

2.2 Characterization

The phase compositions of samples were determined by Bruker D8 Advance X-ray diffraction (XRD). Infrared spectroscopy (IR) studies were performed with Nicolet 5700 infrared spectrometer in the wavenumber range of 4000-400 cm^{-1}.

3 Nonhydrolytic sol-gel method

Nonhydrolytic Sol-Gel process (NHSG) was formally proposed in the early 90s of last century by R. J. P. Corriu of Montpelier University, France (see Corriu, Leclercq, Lefevre, Mutin, & Vioux, 1992). NHSG method forms gel directly from the polycondensation of precursor materials without the hydrolysis or the formation of M-OH.

Compared with the traditional hydrolytic sol-gel method (HSG), NHSG not only simplifies the process, the precursors are also easily to form M-O-M' bond through heterogeneous condensation, achieving atomic uniform mixing, so the short-range ordered gel structure will crystallize by local diffusion at low heating temperature. It can greatly reduce the synthesis temperature of multicompent oxides. For example, NHSG method can synthesize aluminum titanate at 750 ℃ (Feng, Jiang, Liu, Zhang, Hu, & Miao, 2017), while the synthesis temperature for aluminum titanate prepared via traditional hydrolytic sol-gel method (HSG) without strict controlling on hydrolysis rate is 1300 ℃. Therefore, NHSG has become a hot topic in the field of material preparation in the world for its outstanding merits.

3.1 Reaction mechanism of nonhydrolytic sol-gel method

According to different by-products of polycondensation reaction, there are the following four kinds of polycondensation routes in the preparation of metal oxides via nonhydrolytic sol-gel method. (1) alkyl halide elimination polycondensation ; (2) ether elimination polycondensation; (3) ester elimination polycondensation; and (4) amide elimination polycondensation (see Dr, & Markus, 2008; Niederberger, 2007).

Scheme 1 Alkyl halide elimination polycondensation

$$RO-M + M'-X \longrightarrow M-O-M' + RX \qquad (1)$$

Scheme 2 Ether elimination polycondensation

$$M-OR + RO-M' \longrightarrow M-O-M' + ROR \qquad (2)$$

Scheme 3 Ester elimination polycondensation

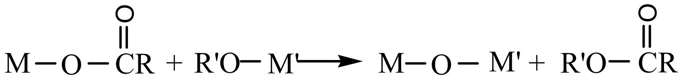

$$M-O-\overset{\overset{O}{\|}}{C}R + R'O-M' \longrightarrow M-O-M' + R'O-\overset{\overset{O}{\|}}{C}R \qquad (3)$$

Scheme 4 Amide elimination polycondensation

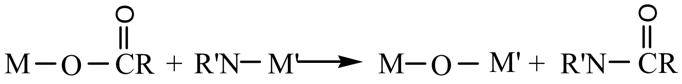

$$M-O-\overset{\overset{O}{\|}}{C}R + R'N-M' \longrightarrow M-O-M' + R'N-\overset{\overset{O}{\|}}{C}R \qquad (4)$$

3.2 Reaction process of nonhydrolytic sol-gel process

Taking alkyl halide elimination polycondensation scheme as an example, the nonhydrolytic sol-gel reaction process is as follow. First, alkyl oxide coordinates with metal ion of metal halide through its lone pair electrons oxygen atom. Then, the nucleophile X^- nucleophillic attack the alkyl carbon atom linked to oxygen atom through the following three possible substitution mechanisms (unimolecular nucleophilic substitution S_N1, bimolecular nucleophilic substitution S_N2 and intramolecular nucleophilic substitution). This nucleophillic attack breaks the carbon-oxygen bond C-O and forms M-O-M' and alkyl halide RX. The specific process is shown in Figure 1 (Feng, 2009). As can be seen from figure 1, to ensure the formation of M-O-M' bond after nucleophilic substitution, nucleophilic X and metal base M' should be closely linked before nucleophilic reaction, so as to ensure the metal base M' can rapidly replace the leaving group after nucleophilic attack to form M-O-M' bond. This requires that the raw material M-A and M'- B exists mianly in the form of covalent bonds, that is ionic character percentage should not be too high.

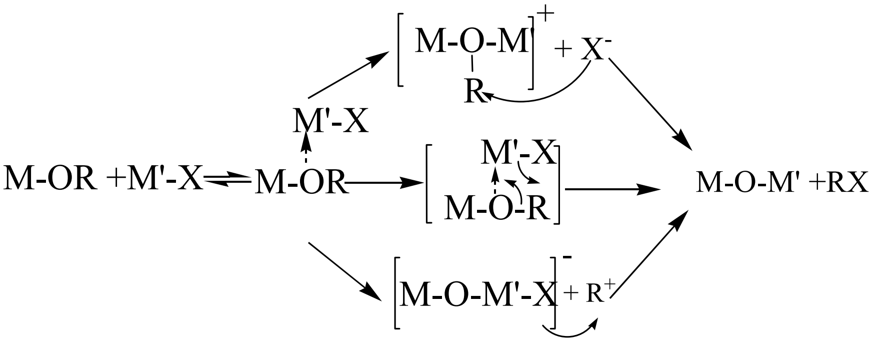

Figure 1 Reaction process of nonhydrolytic sol-gel process for alkyl halide elimination polycondensation

4. Ionic character percentage calculation

Chemical bond is an important index to study the molecular structures and properties. Characteristic of chemical bonds is the motion reflection of the bonded atom's valence electron. This reflection can be inferred by different methods. Fijans proposed the ionic character estimation through dipole moment (Fajans, 1941). Pauling put forward relative electronegativity of elements. He defined element electronegativity as the ability of atom to attract electron and developed thermochemical quantitative estimation method for electronegativity (Pauling, 1932). Pauling proposed that the bigger the electronegativity difference ΔX_{AB} of the two elements in compound AB is, so their electronic attract ability difference is greater. The ionic character percentage is also bigger. Pauling asserted that when the electronegativity difference $\Delta X_{AB} > 1.5$, the chemical bond was ionic bond, and it was covalent bond when the electronegativity difference $\Delta X_{AB} < 1.5$ (Pauling, 1932). It is widely accepted to use electronegativity difference to evaluate the bond character, but there are many exceptions. Different researchers proposed many different onic character percentage calculation model from different views (Isotani, & Watari, 1976; Warhurst, 1951).

The currently widely accepted ionic character percentage calculation model is shown in equation (5)(Pauling, 1967).

$$\text{Ionic character percentage (\%)} = 1-\exp[-(X_A-X_B)^2/4] \qquad (5)$$

In the formula, X_A and X_B are the electronegativity of two atoms in the compound AB

5. Applications of ionic character percentage calculation in nonhydrolytic sol-gel method

5.1 Application in low-temperature synthesis of cordierite via nonhydrolytic sol-gel method

Figure 2 shows the XRD patterns of samples for cordierite synthesis with different magnesium sources of anhydrous $MgCl_2$ ($M_1^{\#}$) and $Mg(OOCCH_3)_2$ ($M_2^{\#}$) calcined at 1200 ℃. Figure 2 shows that no diffraction peak has been detected in sample $M_1^{\#}$, which demonstrates cordierite has not synthesized using $MgCl_2$ as magnesium source. In sample $M_2^{\#}$ with $Mg(OOCCH_3)_2$ as magnesium source, all diffraction peaks belong to α-cordierite phase, which indicates that it has synthesized pure phase of α-cordierite.

In order to reveal the fundamental reason for the influence of magnesium sources on the cordierite synthesis, figure 3 presents the FT-IR patterns of gels prepared using anhydrous $MgCl_2$ (M_1#) and $Mg(OOCCH_3)_2$ (M_2#) as magnesium sources, and table 1 lists the vibration peaks assignments of samples. Figure 3 and table1 indicates that the Al-O-Si, Mg-O-Al and Mg-O-Si bonds appear as 469 cm^{-1}, 681 cm^{-1} and 1580 cm^{-1} in sample M_2# when $Mg(OOCCH_3)_2$ is used as magnesium source. However, when anhydrous $MgCl_2$ is used as magnesium source, although Al-O-Si bond appears at 468.1 cm^{-1} and 466.7 cm^{-1}, Mg-O-Al and Mg-O-Si bonds do not appear. These results indicate that anhydrous $MgCl_2$ does not react with heterogeneous polymerization reaction product of aluminium ethoxide (formation process shown in equation (5)) and tetraethoxysilane (TEOS) (reaction process shown in equation (6)).

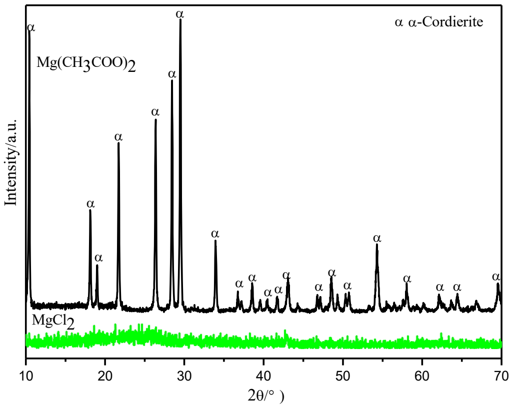

Figure 2 XRD patterns of samples for cordierite synthesis prepared with different magnesium sources

The fundamental reasons for the results above are as follows. When anhydrous $MgCl_2$ is used as magnesium source, magnesium is alkaline earth metal element, and its electronegativity is 1.31. Chloride is the halogen element, and its electronegativity is

3.16. The ionic character percentages of Mg-Cl bond is calculated to be 57.50 % according to formula (5), which indicates that anhydrous $MgCl_2$ has obvious ionic character. Anhydrous $MgCl_2$ tends to exist in the form of ions in ethanol solution. Therefore, alkyl halide elimination polycondensation fails. When anhydrous magnesium acetate is used as magnesium source, ester elimination polycondensation between anhydrous magnesium acetate and TEOS (shown in equation (7)), anhydrous magnesium acetate and aluminium ethoxide (shown in equation (7)) can occur with the formation of Mg-O-Si and Mg-O-Al bonds. This ensures that cordierite can be synthesized at low temperature by taking anhydrous magnesium acetate as magnesium source.

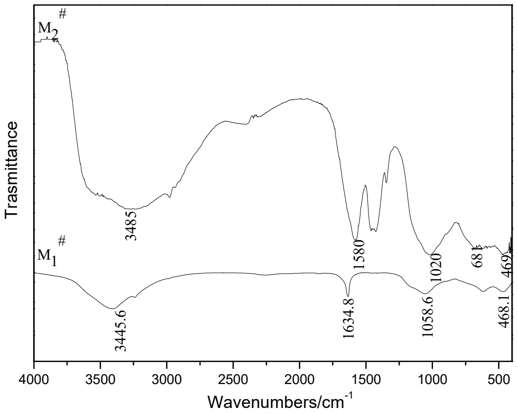

Figure 3 Infrared spectra of xerogels for cordierite synthesis prepared with different magnesium sources

Table1 Infrared vibration peaks attribution of xerogels for cordierite synthesis prepared with different magnesium sources

Category	M_1#	M_2#	Attribution	References
Peak position /cm^{-1}	468.1	469	Al-O-Si	(see Rayalu, Udhoji, Meshram, Naidu, & Devotta, 2005; Clayden, Esposito, Aronne, & Pernice, 1999)
		681	Mg-O-Al	(see Petrovic, Janackovic, Bozovic, & Zec, 2001)
	1058	1020	Si-O-Si	(see Corriu, Leclercq, Lefèvre, Mutin, & Vioux, 1992; Gupta, Dillon, Bracker, & George, 1991)
		1580	Mg-O-Si	(see Akcay, 2004)
	1634.8	1662.1	C=O	(see Pessoa, Ignacio, Pessoa, M.C. D., Araya, Fajardo, & Barría, 2011; Chtourou, Abdelhédi, Frikha, & Trabelsi, 2010)
	3445.6	3485	-OH	(see Huang, Zhang, Yi, Tang, Zhang, & Su, 2014; Fan, Bi, & Li, 2002)

$$2Al + 6C_2H_5OH \xrightarrow{I_2} 2Al(OC_2H_5)_3 + 3H_2 \qquad (5)$$

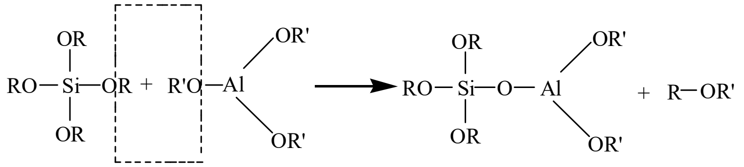
(6)

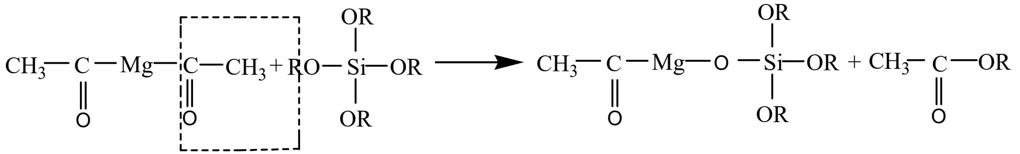
(7)

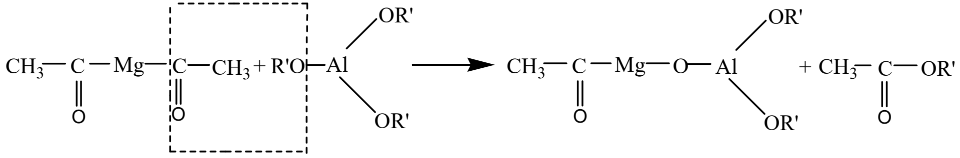
(8)

R= R′=C_2H_5

5.2 Application in low-temperature synthesis of magnesium-stabilized aluminum titanate via nonhydrolytic sol-gel method

Figure 4 depicts the XRD patterns of magnesium-stabilized aluminum titanate samples with magnesium fluoride (M_1#), anhydrous magnesium acetate (M_2#) and magnesium ethoxide (M_3#) as stabilizers and without stabilizer (W#). As shown in

Figure 4, with the addition of Mg-stabilizer, aluminum titanate sample is worse compared with the sample without stabilizer ($W^{\#}$), which is indicated by the decrease of relative intensity of aluminum titanate diffraction peaks. Almost no aluminum titanate diffraction peaks are detected in samples $M_1^{\#}$, and the diffraction peaks intensity of corundum and rutile in these two samples is much higher than that of other samples. It is mainly due to the strong polarity of MgF_2. Its ionic character percentage is calculated to be 85.9%. MgF_2 exists in the system in the form of ions. Magnesium ions act as strong Lewis acid, they can promote the homogeneous polycondensation nonhydrolytic reaction. The main crystal phase of samples $M_2^{\#}$, $M_3^{\#}$ and $W^{\#}$ is aluminum titanate. However, the aluminum titanate peaks positions in $M_2^{\#}$ and $M_3^{\#}$ shifts to the lower angle relative to sample $W^{\#}$ and the standard PDF card of aluminum titanate, and they are burr with shouldered peaks, these indicate that magnesium has doped into the lattice of aluminum titanate.

In order to reveal the Mg-stabilizers effect on aluminum titanate, samples $W^{\#}$ (without stabilizer), $M_1^{\#}$(magnesium fluoride as stabilizer) and $M_3^{\#}$(magnesium ethoxide as stabilizer) were chosen for FT-IR analysis. The results are shown in figure 5. It indicates that the most obvious difference between samples $W^{\#}$ and $M_2^{\#}$ is that the Al-O-Ti heterogeneous vibration peak disappeared in FT-IR spectrum of sample $M_3^{\#}$. Therefore, there is almost no aluminum titanate phase in its XRD pattern at 750 ºC. And the differences between the IR spectra of samples $M_3^{\#}$ and $W^{\#}$ are as follows, Ti-O-Mg bond at 889 cm^{-1} (see Bradley, Hancock, & Wardlaw, 1952), Al-O-Mg at 678 cm^{-1} and 786 cm^{-1} appeared (see Nembenna, Roesky, Mandal, Oswald, Pal, &

Herbstirmer, 2006), meanwhile there are Ti-O-Ti (Stanciu, Groza, Jitianu, & Maria, 2004) and Al-O-Al (Sawata, Komiyama, & Taira, 1995) bonds at 482 cm^{-1} and 1070 cm^{-1}, respectively. The formation of Ti-O-Mg and Al-O-Mg is mainly due to that the alkoxy in magnesium ethoxide can replace ethyl in $M(OEt)_xCl_y$ (M = Al or Ti, the intermediate of the reaction between anhydrous ethanol and titanium tetrachloride or anhydrous aluminium chloride), to form M-O-Mg (M =Al or Ti) bonds, the reaction is shown in equation (9) and equation (10).

Similarly, magnesium acetate can react with the alkyl in $M(OEt)_xCl_y$ (M =Al or Ti), to form M-O-Mg bonds through ester elimination polycondensation, which is shown in equation (11).

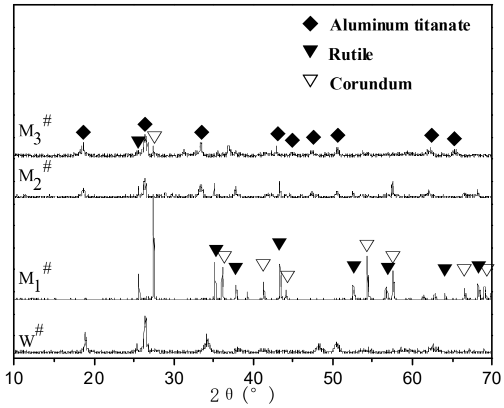

Figure 4 XRD patterns of samples for magnesium-stabilized aluminum titanate synthesisprepared with different magnesium sources

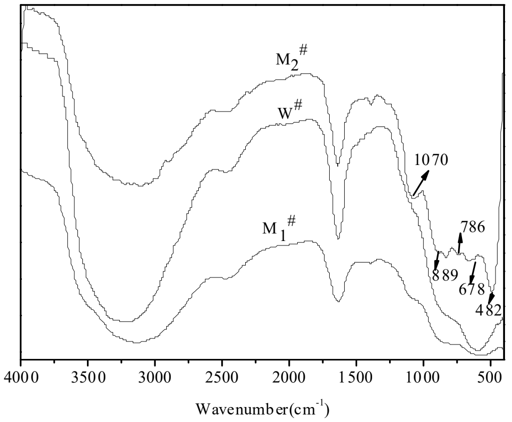

Figure 5 FT-IR patterns of samples for magnesium-stabilized aluminum titanate synthesis prepared with different

magnesium sources

$$(EtO)_xCl_yM + Mg(OEt)_2 \longrightarrow (EtO)_{x-1}Cl_yM\text{- }O\text{-}Mg(OEt) + EtOEt \quad (9)$$

$$(EtO)_xCl_yM + Mg(OEt)_2 \longrightarrow (EtO)_xCl_{y-1}M\text{- }O\text{-}Mg(OEt) + EtCl \quad (10)$$

$$(EtO)_xCl_yM + Mg(OOCCH_3)_2 \longrightarrow (EtO)_{x-1}Cl_yM\text{- }O\text{-}Mg(OOCCH_3) + EtOOCCH_3 \quad (11)$$

(M = Al or Ti, x + y = 3 or 4)

Conclusions

As a typical nucleophilic substitution reaction process, one of the keys for nonhydrolytic polycondensation reaction to form heterogeneous M-O-M' bond is the ionic character percentage of nucleophilic reaction raw materials MA and M'B should not be too high (no more than 50%). It is the only way to ensure the metal base can quickly replace the leaving group after nucleophilic attack. It is also one of the basic prerequisites to form M-O-M' bond. Otherwise, the metal base linked to the nucleophile will be enriched among the networks in the form of ions. Of course, the raw material selected should first meet the nonhydrolytic polycondensation reaction mechanisms. These are the basic principles for the formation of heterogeneous M-O-M' bond by nonhydrolytic heteropolycondensation reaction and the realization of atomic uniform mixing of precursor materials.

Acknowledgements

This work was supported by the National Natural Science Foundation of China [grant numbers 51162013, 51362014]; the Major Discipline Academic and Technical Leader Training Plan Project of Jiangxi Province [grant number 20113BCB22009]; the Science and Technology Supporting Plan Project of Jiangxi Province, China [grant number 20111BBE50018]; the Youth Science Foundation of Jiangxi Province, China [grant number 20171BAB216009]; the Science Foundation of Jiangxi Provincial Department of Education, China [grant number GJJ150887]; the Youth Science Foundation of Jiangxi Provincial Department of Education, China [grant number GJJ150892]; the Post Doctoral researchers preferred funded projects of Jiangxi Province [grant number 2013KY34]; and the Jingdezhen Science and technology program [grant number 20161GYZD011-007].

References

Akcay, M. (2004). FT-IR spectroscopic investigation of the adsorption pyridine on the raw sepiolite and Fe-pillared sepiolite from anatolia. Journal of molecular structure, 694(1), 21-26. https://doi.org/10.1016/j.molstruc.2004.01.010.

Andrianainarivelo, M., Corriu, R. J. P., Leclercq, D., And, P. H. M., & Vioux, A. (1997). Nonhydrolytic sol−gel process: aluminum titanate gels. Chemistry of materials, 9(5), 1098-1102. https://doi.org/10.1039/jr9520002773.

Arnal, P., Corriu, R. J. P., Leclercq, D., And, P. H. M., & Vioux, A. (1997). A solution chemistry study of nonhydrolytic sol−gel routes to titania. Chemistry of materials. 9(3), 694-698. https://doi.org/ 10.1021/cm960337t.

Bradley, D. C., Hancock, D. C., & Wardlaw, W. (1952). 524. Titanium chloride alkoxides. Journal of the chemical society, 2773-2778. https://doi.org/ 10.1039/JR9520002773

Chtourou, M., Abdelhédi, R., Frikha, M. H., & Trabelsi, M. (2010). Solvent free synthesis of 1,3-diaryl-2-propenones catalyzed by commercial acid-clays under ultrasound irradiation. Ultrasonics sonochemistry, 17(1), 246-249. https://doi.org/

10.1016/j.ultsonch.2009.06.008

Clayden, N. J., Esposito, S., Aronne, A., & Pernice, P. (1999). Solid state 27 Al NMR and FTIR study of lanthanum aluminosilicate glasses. Journal of Non-Crystalline Solids, 258(1–3), 11-19. https://doi.org/10.1016/S0022-3093(99)00555-4

Corriu, R. J. P., Leclercq, D., Lefevre, P., Mutin, P. H., & Vioux, A. (1992). Preparation of monolithic gels from silicon halides by a non-hydrolytic sol-gel process. Journal of non-crystalline solids, 146(2-3), 301-303. https://doi.org/10.1016/S0022-3093(05)80505-8

Dr, N. P., & Markus, N. (2008). Surfactant-free nonaqueous synthesis of metal oxide nanostructures. Angewandte chemie international edition, 47(29), 5292-304. https://doi.org/ 10.1002/anie.200704541.

Fajans, K. (1941). Polarization of ions and lattice distances. Journal of chemical physics, 9(3), 281-282. https://doi.org/10.1063/1.4918971

Fan, Y., Bi, C., & Li, J. (2002). Synthesis and characterization of UO_2 (ii) and th(iv) binuclear complexes with o-vanillylidene anthranilic acid. Journal of radioanalytical & nuclear chemistry, 254(3), 641-644. https://doi.org/ 10.1023/A:1021761814314

Feng, G., Jiang, W. H., Liu, J. M., Zhang, Q., Hu, Z., & Miao, L. F. (2016). Low-temperature synthesis of magnesium-stabilized aluminum titanate powder via non-hydrolytic sol-gel method. Materials science forum. 848(1), 319-323. https://doi.org/10.4028/www.scientific.net/MSF.848.319

Feng, G., Jiang, W. H., Liu, J. M., Li, C., Zhang, Q., Miao, L. F & Wu, Q. (2017).

Novel nonaqueous precipitation synthesis of alumina powders. Ceramics international. 43(16), 13461-13468. https://doi.org/10.1016/j.ceramint.2017.07.050

Feng, G., Jiang, W., Liu, J., Zhang, Q., Wu, Q., & Miao, L. (2017). A novel green nonaqueous sol-gel process for preparation of partially stabilized zirconia nanopowder. Processing and application of ceramics. 11(3), 220-224. https://doi.org/10.2298/PAC1703220F

Feng, G., Jiang, W. H., Liu, J. M., Zhang, Q., Hu, Z., & Miao, L. F. (2017). Effects of anhydrous magnesium acetate's addition time on low- temperature synthesis of magnesium-stabilized aluminum titanate powder via non-hydrolytic sol-gel method. Journal of ceramics. 38(4), 471-475. https://doi.org/10.13957/j.cnki.tcxb.2017.04.004

Feng, G., Zhou, X. M., Jiang, W. H., Liu, J. M., Zhang, Q., Hu, Z., & Miao, L. F. (2017). Research on reaction process of synthesis of cordierite via nonhydrolytic sol-gel method. China ceramics. 53(4), 46-51. https://doi.org/10.16521/j.cnki.issn.1001-9642.2017.04.0

Feng, G., Zhou, X. M., Jiang, W. H., Liu, J. M., Zhang, Q., Hu, Z., & Miao, L. F. (2017). Effects of mineralizer on synthesis of cordierite powder via non-hydrolytic sol-gel method. China ceramics. 53(4), 46-51. https://doi.org/10.16521/j.cnki.issn.1001-9642.2017.11.010

Feng, G. (2009). Study on the preparation of aluminum titanate film via sol-gel method. Jingdezhen Ceramic Institute.

http://kreader.cnki.net/Kreader/CatalogViewPage.aspx?dbCode=cdmd&filename=2010056149.nh&tablename=CMFD2011&compose=&first=1&uid=WEEvREcwSlJHSldRa1FhdkJkVWI2cEg1MXdSdWtJNGJsT0JRLzRxaEE1UT0=$9A4hF_YAuvQ5obgVAqNKPCYcEjKensW4ggI8Fm4gTkoUKaID8j8gFw!!.

Gupta, P., Dillon, A. C., Bracker, A. S., & George, S. M. (1991). FTIR studies of H_2O and D_2O decomposition on porous silicon surfaces. Surface Science, 245(3), 360-372. https://doi.org/10.1016/0039-6028(91)90038-T.

Hamadi, A., & Nabih, K. (2012). Alkali activation of oil shale ash based ceramics. 9(9), 1373-1388. https://doi.org/10.1155/2012/769532

Huang, F., Zhang, R., Yi, Y., Tang, X., Zhang, M., & Su, D., et al. (2014). Comparison of physicochemical properties and immunomodulatory activity of polysaccharides from fresh and dried litchi pulp. Molecules, 19(4), 3909-25. https://doi.org/ 10.3390/molecules19043909 .

Isotani, S., & Watari, K. (1976). An empirical relation between bond distance and the percentage of ionic character. Journal of inorganic & nuclear chemistry, 38(3), 501-505. https://doi.org/10.1016/0022-1902(76)80292-8.

Joo, J., Kwon, S., Yu, J., & Hyeon, T. (2005). Synthesis of ZnO nanocrystals with cone, hexagonal cone, and rod shapes via non‐hydrolytic ester elimination sol–gel reactions. Advanced materials, 17(15), 1873-1877. https://doi.org/10.1002/adma.200402109

Nembenna, S., Roesky, H. W., Mandal, S. K., Oswald, R. B., Pal, A., & Herbstirmer, R. (2006). Soluble molecular compounds with the Mg-O-Al structural motif: a model approach for the fixation of organometallics on a MgO surface. Journal of the american chemical society, 128(40), 13056-13057. https://doi.org/10.1021/ja064460p

Niederberger, N. (2007). Nonaqueous sol–gel routes to metal oxide nanoparticles. Accounts of chemical research. 40(1), 793-800. https://doi.org/ 10.1021/ar600035e.

Pauling, L. (1932). The nature of the chemical bond. iv. the energy of single bonds and the relative electronegativity of atoms. Journal of the American chemical society, 54(9), 3570-3582. https://doi.org/ 10.1021/ja01348a011

Pessoa, M. H., Ignacio, C. M., Pessoa-Mahana, C. D., Araya, M., R., Fajardo, I. A., & Barría, C. S. (2011). Synthesis of 1-benzyl-3-[4-(aryl-1-piperazinyl) carbonyl]-1h-indoles: novel ligands with potential d4 dopaminergic activity. Journal of the Chilean chemical society, 56(4), 866-869. http://dx.doi.org/10.4067/S0717-97072011000400009

Rayalu, S. S., Udhoji, J. S., Meshram, S. U., Naidu, R. R., & Devotta, S. (2005). Estimation of crystallinity in flyash-based zeolite-a using XRD and IR spectroscopy. Current science, 89(12), 2147-2151. http://www.jstor.org/stable/24111077

Sawata, S., Komiyama, M., & Taira, K. (1995). Kinetic evidence based on solvent isotope effects for the nonexistence of a proton-transfer process in reactions catalyzed by a hammerhead ribozyme: implication to the double-metal-ion mechanism of catalysis. Journal of the American chemical society. 117(8), 2357-2358. https://doi.org/10.1021/ja00113a028.

Stanciu, L. A., Groza, J. R., Jitianu, A., & MariaZaharescu. (2004). Structural evolution during reaction to form aluminum titanate from sol-gel precursors. Advanced manufacturing processes, 19(4), 641-650. https://doi.org/10.1081/AMP-200028090

Vioux, A. (1997). Nonhydrolytic sol−gel routes to oxides. Chemistry of Materials, 9(11), 2292-2299. https://doi.org/ 10.1021/cm970322a

Vona, M. L. D., Polini, R., Sebastianelli, P., & Licoccia, S. (2004). A non-hydrolytic sol-gel approach for the preparation of $Mg_xAl_{2(1-x)}Ti_{(1+x)}O_5$, powders. Journal of sol-gel science and technology, 31(1-3), 95-98. https://doi.org/10.1023/B:JSST.0000047967.82122.6f

Warhurst, E. (1951). The ionic character of bonds and bond properties. Proceedings of the royal society of London, 207(1088), 32-49. http://www.jstor.org/stable/98674